Electronic Supplementary Material (ESI)

Highly stable actinide(III) complexes supported by doubly aromatic ligands

Naixin Zhang,[a] Cong-Zhi Wang,[a] Qun-Yan Wu,[a] Jian-Hui Lan,[a] Zhi-Fang Chai,[a,b] and Wei-Qun Shi*[a]*

[a]Laboratory of Nuclear Energy Chemistry, Institute of High Energy Physics, Chinese Academy of Sciences, Beijing 100049, China

[b]Engineering Laboratory of Advanced Energy Materials, Ningbo Institute of Materials Technology and Engineering, Chinese Academy of Sciences, Ningbo 315201, China

Email: shiwq@ihep.ac.cn, wangcongzhi@ihep.ac.cn

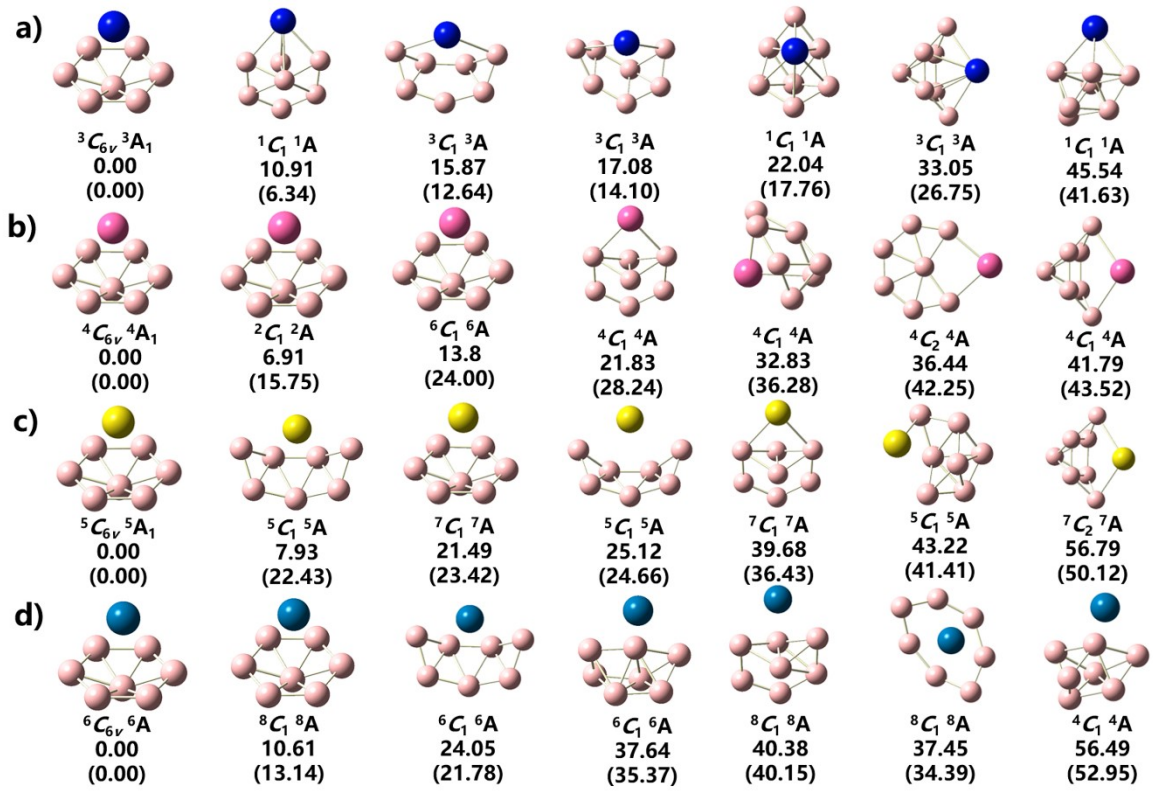

Figure S1. The low-lying isomers of (a) PaB_7, (b) UB_7, (c) NpB_7, and (d) PuB_7 along with the relative energies (in kcal/mol) at the PBE0/6-311+G*/RECP and TPSSh/6-311+G*/RECP (in parentheses) theoretical levels. All the energies are corrected for zero-point energies. Dark blue, pink, yellow, and blue spheres represent B, Pa, U, Np, and Pu, respectively.

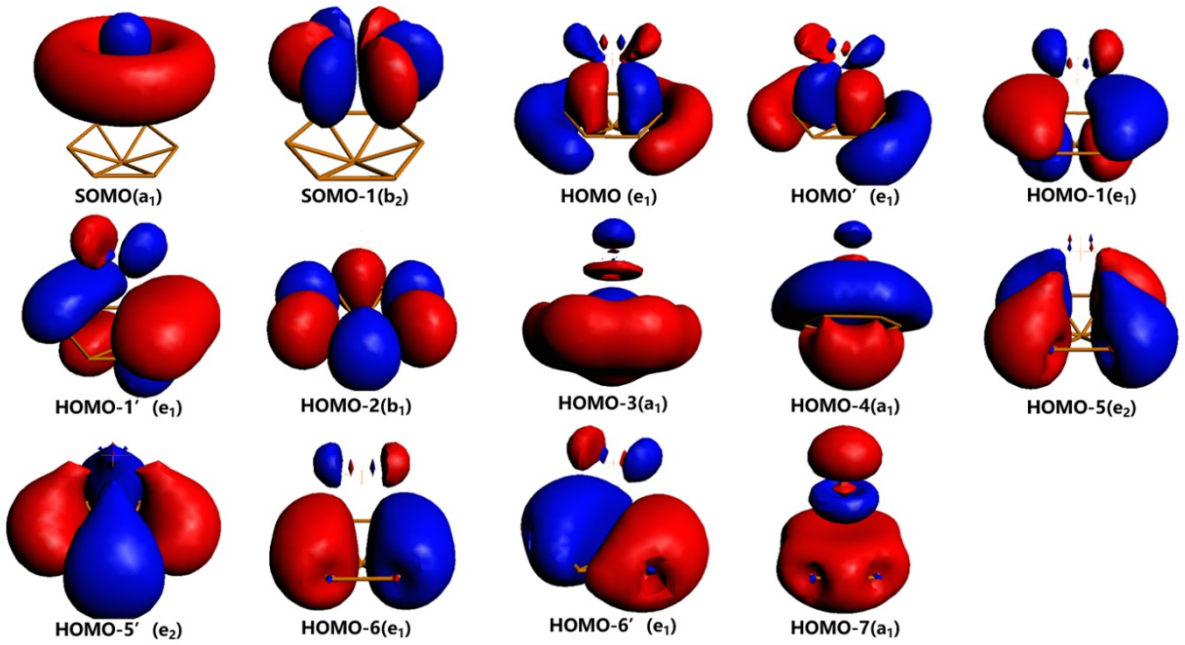

Figure S2. The MOs of PaB_7 at the theoretical level of PBE0/6-311+G*/RECP.

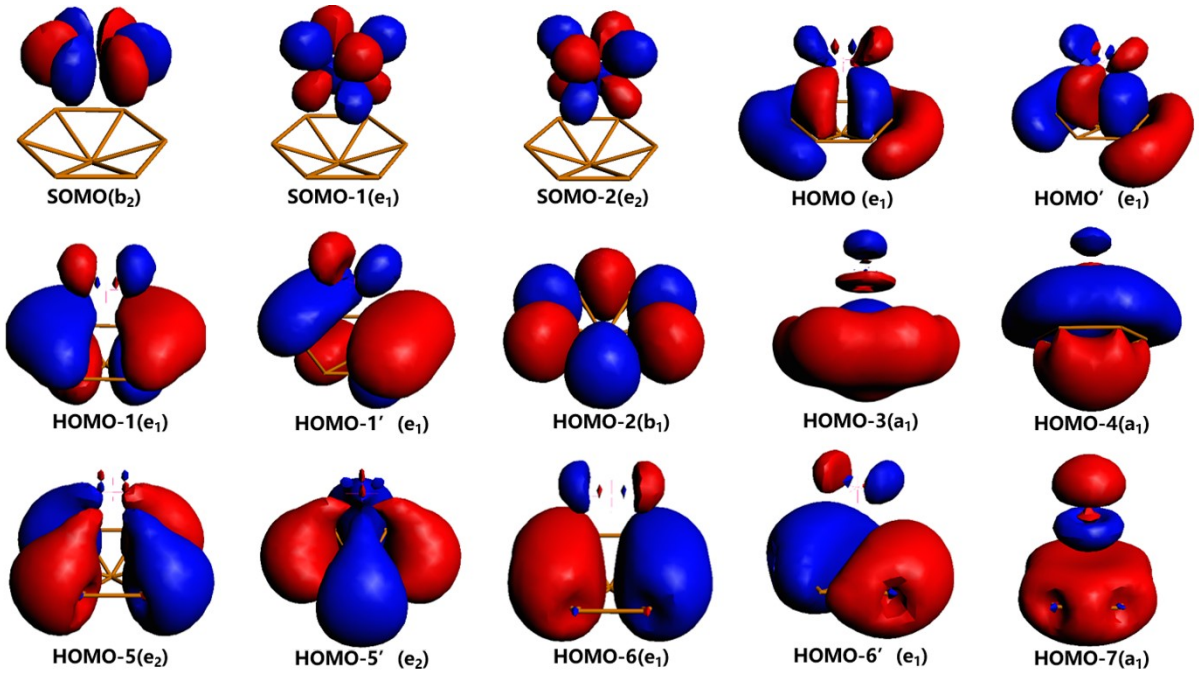

Figure S3. The MOs of UB_7 at the theoretical level of PBE0/6-311+G*/RECP.

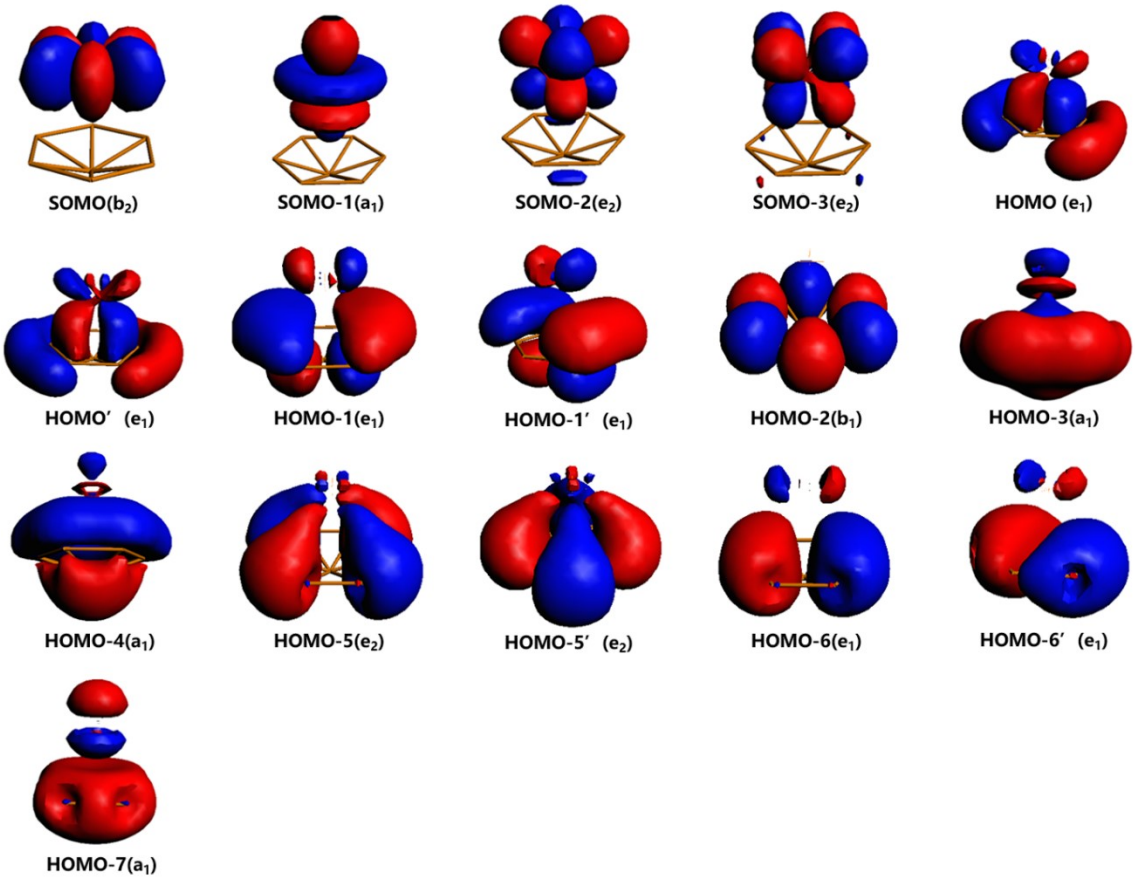

Figure S4. The MOs of NpB_7 at the theoretical level of PBE0/6-311+G*/RECP.

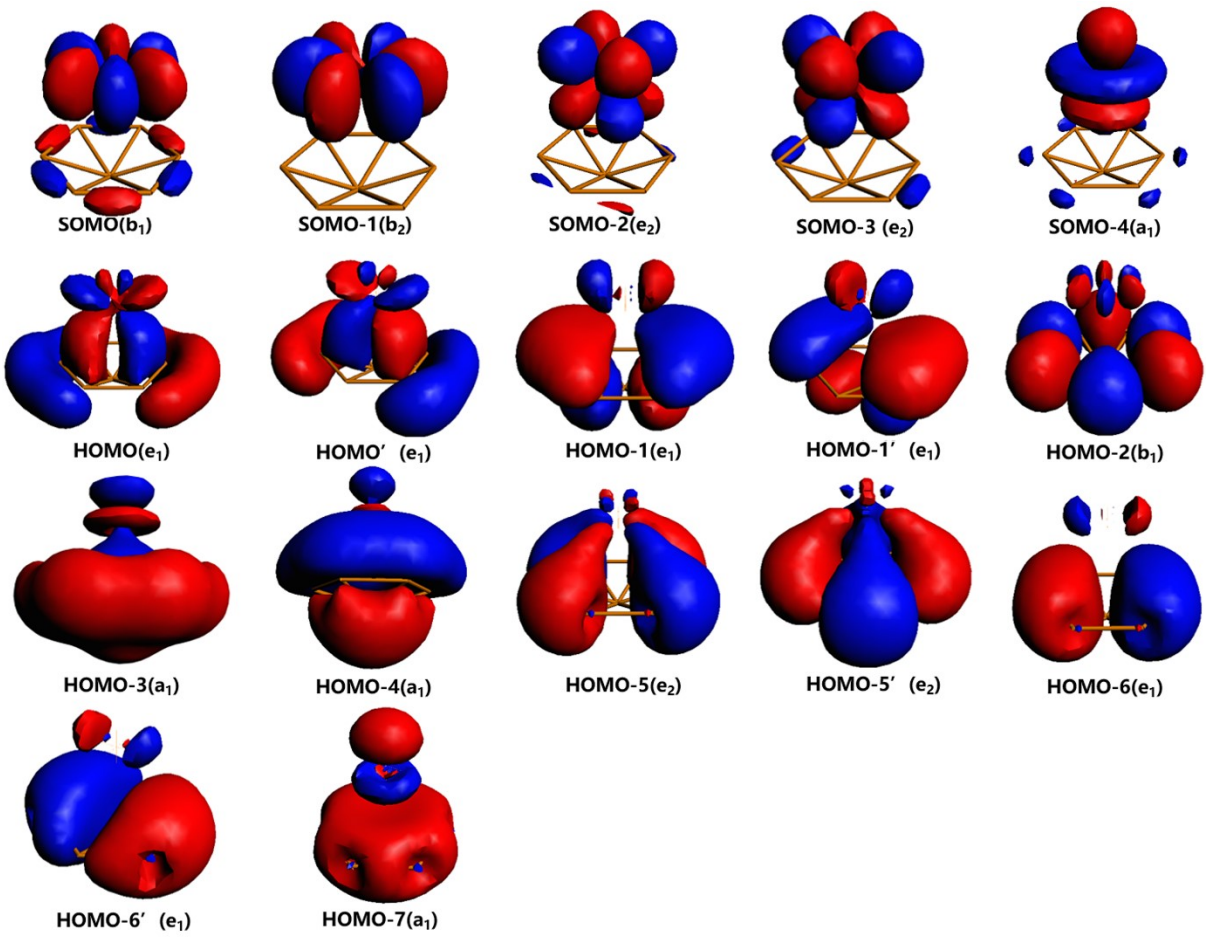

Figure S5. The MOs of PuB_7 at the theoretical level of PBE0/6-311+G*/RECP.

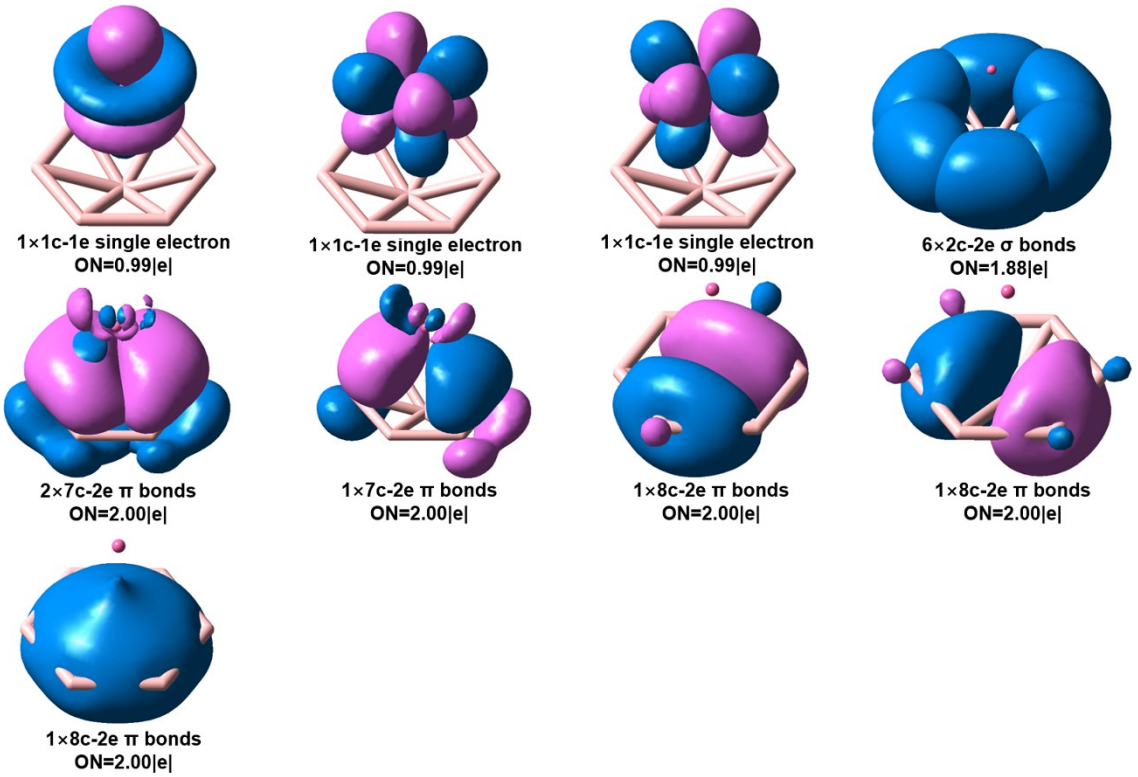

Figure S6. Bonding pattern of C_{6v} UB_7 from AdNDP analysis with the occupation numbers (ONs) at the PBE0/6-311+G*/RECP level of theory.

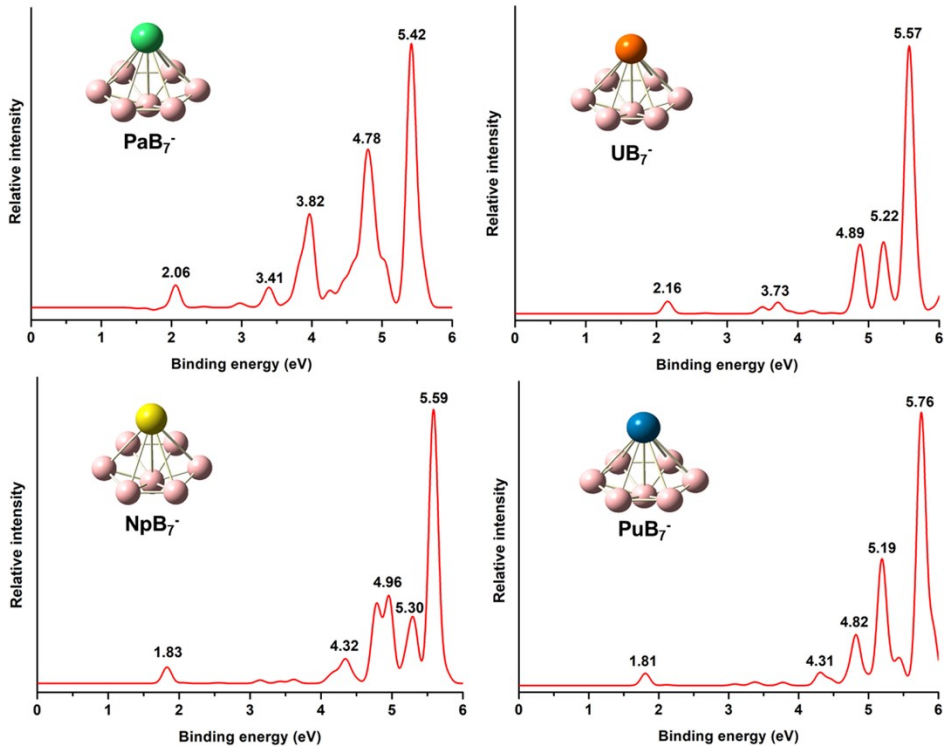

Figure S7. The simulated photoelectron spectrum of AnB_7^- at the PBE0/6-311+G*/RECP level of theory.

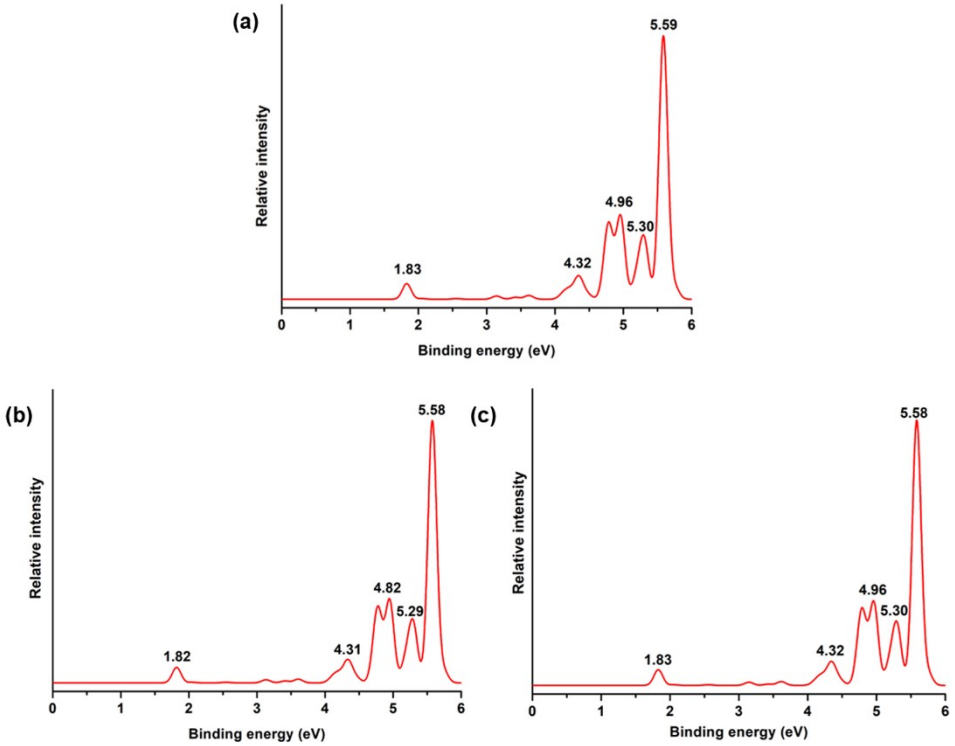

Figure S8. The simulated photoelectron spectrum of NpB_7^- at the (a) PBE0/6-311+G*/RECP, (b) PBE0/6-311++G*/RECP, and (c) PBE0/6-311+G(2df, p)/RECP theoretical levels.

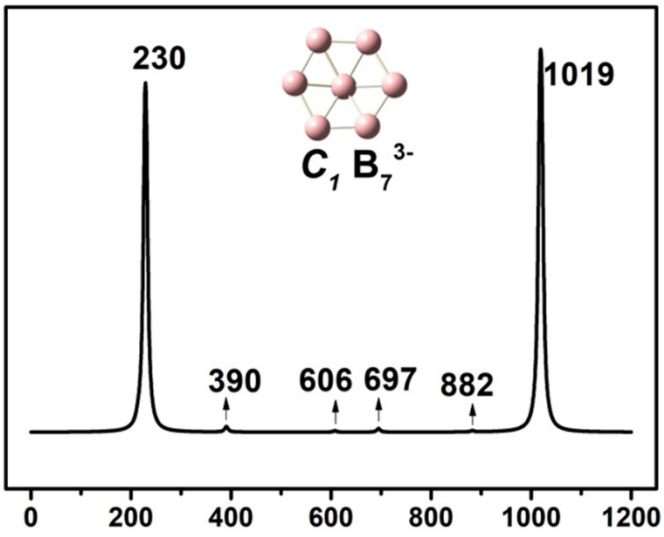

Figure S9. The infrared spectra of B_7^{3-} at the PBE0/6-311+G*/RECP level of theory.

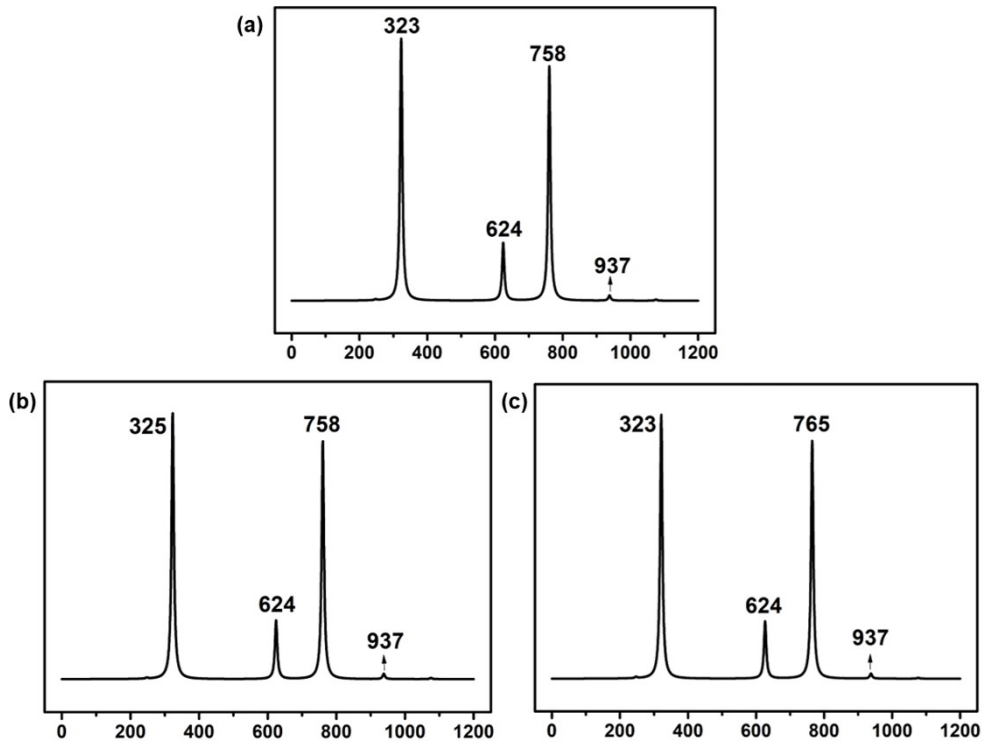

Figure S10. The infrared spectra of NpB_7 at the (a) PBE0/6-311+G*/RECP, (b) PBE0/6-311++G*/RECP, and (c) PBE0/6-311+G(2df, p)/RECP theoretical levels.

Table S1. Theoretical harmonic vibrational frequencies (in cm^{-1}) for the global minimum structures of AnB_7 by the PBE0 method (infrared intensities in parentheses are in km/mol).

$PaB_7(C_{6v})$	$UB_7(C_{6v})$	$NpB_7(C_{6v})$	$PuB_7(C_{6v})$
222.5 (e_1, 0.1)	259.9 (e_1, 0.0)	247.6 (e_1, 0.1)	241.3 (e_1, 0.1)
222.5 (e_1, 0.1)	259.9 (e_1, 0.0)	247.7 (e_1, 0.1)	241.3 (e_1, 0.1)
328.5 (a_1, 73.0)	323.3 (a_1, 43.2)	323.1 (a_1, 50.6)	307.8 (a_1, 42.9)
484.4 (b_2, 0.0)	478.6 (e_2, 0.0)	492.4 (b_2, 0.0)	489.5 (e_2, 0.0)
508.8 (e_2, 0.0)	478.6 (e_2, 0.0)	493.6 (e_2, 0.0)	489.5 (e_2, 0.0)
508.8 (e_2, 0.0)	481.8 (b_2, 0.0)	493.6 (e_2, 0.0)	492.8 (b_2, 0.0)
630.8 (a_1, 20.0)	621.7 (a_1, 11.8)	624.4 (a_1, 11.1)	616.8 (a_1, 14.1)
665.2 (e_2, 0.0)	680.3 (e_2, 0.0)	678.6 (e_2, 0.0)	672.7 (e_2, 0.0)
665.2 (e_2, 0.0)	680.3 (e_2, 0.0)	678.6 (e_2, 0.0)	672.7 (e_2, 0.0)
733.2 (b_2, 0.0)	740.5 (b_2, 0.0)	744.6 (b_2, 0.0)	737.2 (b_2, 0.0)
762.0 (e_1, 20.0)	763.7 (e_1, 26.7)	760.5 (e_1, 22.6)	760.1 (e_1, 19.5)
762.0 (e_1, 20.0)	763.7 (e_1, 26.7)	760.5 (e_1, 22.7)	760.1 (e_1, 19.5)
933.1 (a_1, 0.0)	937.4 (a_1, 0.7)	938.2 (a_1, 1.0)	940.5 (a_1, 1.0)
1073.8 (e_1, 0.6)	1073.8 (b_1, 0.0)	1075.4 (e_1, 0.1)	1075.6 (e_1, 0.1)
1073.8 (e_1, 0.6)	1078.7 (e_1, 0.0)	1075.4 (e_1, 0.1)	1075.6 (e_1, 0.1)
1077.3 (b_1, 0.0)	1078.7 (e_1, 0.0)	1090.7 (b_1, 0.0)	1117.5 (b_1, 0.0)
1155.9 (e_2, 0.0)	1153.6 (e_2, 0.0)	1161.1 (e_2, 0.0)	1152.1 (e_2, 0.0)
1155.9 (e_2, 0.0)	1153.6 (e_2, 0.0)	1161.1 (e_2, 0.0)	1152.1 (e_2, 0.0)

Table S2. The EDA results (kcal/mol) of AnB_7 at the PBE/TZP/ZORA level of theory. The values in parentheses indicate the percentage of each value relative to the sum of the values ($\Delta E_{elstat} + \Delta E_{orb}$).

Species	ΔE_{Pauli}	ΔE_{elstat}	ΔE_{orb}	ΔE_{int}
C_{6v} PaB_7	459.90	-1107.87(56.8%)	-841.94(43.2%)	-1489.91
C_{6v} UB_7	477.15	-1119.69(49.0%)	-1164.48(51.0%)	-1807.01
C_{6v} NpB_7	482.03	-1124.25(46.5%)	-1294.14(53.5%)	-1936.36
C_{6v} PuB_7	442.07	-1104.30(50.5%)	-1081.88(49.5%)	-1744.11

Table S3. QTAIM analysis of AnB_7, density of electrons ρ, Laplacian of electron density $\nabla^2\rho$, energy density H, and the total delocalization index (DI_{total}) of the An-B bonds at the PBE0/6-311+G*/RECP level.

Species	ρ	$\nabla^2\rho$	H	DI_{total}
C_{6v} PaB_7	0.0667	0.0715	-0.01907	3.0185
C_{6v} UB_7	0.0653	0.0942	-0.01827	2.9541
C_{6v} NpB_7	0.0664	0.0961	-0.01871	3.0187
C_{6v} PuB_7	0.0638	0.0950	-0.01736	3.0099

Table S4. The molecular orbital composition analysis of Pa for PaB_7 at the theoretical level of PBE0/6-311+G*/RECP.

Species	Orbital	7s	7p	6d	5f
PaB_7	SOMO			49.09	23.43
	SOMO-1		0.62	9.44	6.42
	HOMO		0.56	9.30	5.68
	HOMO′				97.17
	HOMO-1		2.28	19.58	
	HOMO-1′		2.21	19.06	
	HOMO-2				0.64
	HOMO-3			8.64	0.63
	HOMO-4	27.78	0.64		
	HOMO-5			3.06	0.78
	HOMO-5′			4.71	2.23
	HOMO-6		0.73	3.52	
	HOMO-6		0.73	3.48	
	HOMO-7	4.41	9.92	2.22	

Table S5. The molecular orbital composition analysis of U for UB_7 at the theoretical level of PBE0/6-311+G*/RECP.

Species	Orbital	7s	7p	6d	5f
UB_7	SOMO			10.80	4.54
	SOMO-1			10.80	4.54
	SOMO-2			2.18	93.31
	HOMO			2.18	93.31
	HOMO′	3.21	0.73	6.61	88.70
	HOMO-1		2.69	15.62	
	HOMO-1′		2.69	15.62	
	HOMO-2				0.80
	HOMO-3			5.84	3.58
	HOMO-4	25.99	0.75		
	HOMO-5			3.07	3.48
	HOMO-5′			3.07	3.48
	HOMO-6		0.83	3.5	
	HOMO-6		0.83	3.5	
	HOMO-7	3.37	11.59	1.15	

Table S6. The molecular orbital composition analysis of Np for NpB_7 at the theoretical level of PBE0/6-311+G*/RECP.

Species	Orbital	7s	7p	6d	5f
NpB_7	SOMO			9.83	7.71
	SOMO-1			9.83	7.71
	SOMO-2			1.42	93.51
	SOMO-3			1.42	93.51
	HOMO	1.47		4.49	86.49
	HOMO′				98.90
	HOMO-1		2.41	14.69	
	HOMO-1′		2.41	14.69	
	HOMO-2				0.75
	HOMO-3			5.41	7.43
	HOMO-4	26.56	0.65		2.96
	HOMO-5			2.98	4.52
	HOMO-5′			2.98	4.52
	HOMO-6		0.78	3.60	0.51
	HOMO-6		0.78	3.60	0.51
	HOMO-7	4.52	9.73	1.86	

Table S7. The molecular orbital composition analysis of Pu for PuB_7 at the theoretical level of PBE0/6-311+G*/RECP.

Species	Orbital	7s	7p	6d	5f
	SOMO			7.36	17.45
	SOMO-1			7.36	17.45
	SOMO-2				90.32
	SOMO-3				98.90
	SOMO-4			0.66	93.66
	HOMO			0.66	93.66
	HOMO′		2.19	13.29	
	HOMO-1		2.19	13.29	
PuB_7	HOMO-1′	0.88		4.83	75.19
	HOMO-2				9.95
	HOMO-3			4.00	18.31
	HOMO-4	26.22	1.12		4.58
	HOMO-5			2.54	5.03
	HOMO-5′			2.54	5.03
	HOMO-6		0.71	3.28	0.53
	HOMO-6		0.71	3.28	0.53
	HOMO-7	5.34	8.61	1.98	

Table S8. The calculated vertical detachment energies (VDEs) for PaB_7^- at the PBE0/6-311+G*/RECP level of theory.

VDE	Final state and electron configuration
2.06	$^3A_1\{\ldots 6b_1^2 6b_2^2 7b_1^2 7b_2^2 8b_1^2 8b_2^1 4a_2^1 \mathbf{14a_1^0}\}$
3.41	$^3A_1\{\ldots 6b_1^2 6b_2^2 7b_1^2 7b_2^2 8b_1^2 \mathbf{8b_2^0} 4a_2^1 14a_1^1\}$
3.82	$^5B_1\{\ldots 6b_1^2 6b_2^2 \mathbf{7b_1^1} 7b_2^2 8b_1^2 8b_2^1 4a_2^1 14a_1^1\}$
4.78	$^5A_1\{\ldots \mathbf{6b_1^1} 6b_2^2 7b_1^2 7b_2^2 8b_1^2 8b_2^1 4a_2^1 14a_1^1\}$
5.42	$^5A_2\{\ldots 6b_1^2 6b_2^2 7b_1^2 \mathbf{7b_2^1} 8b_1^2 8b_2^1 4a_2^1 14a_1^1\}$

Table S9. The calculated VDEs for UB_7^- at the PBE0/6-311+G*/RECP level of theory.

VDE	Final state and electron configuration
2.16	$^4A_1\{\ldots 5b_1^2 6b_1^2 7b_2^2 14a_1^2 15a_1^1 4a_2^1 7b_1^1 \mathbf{8b_2^0}\}$
3.73	$^4A_2\{\ldots 5b_1^2 6b_1^2 7b_2^2 14a_1^2 15a_1^1 \mathbf{4a_2^0} 7b_1^1 8b_2^1\}$
4.89	$^4A_1\{\ldots 5b_1^2 6b_1^2 7b_2^2 14a_1^2 \mathbf{15a_1^0} 4a_2^1 7b_1^1 8b_2^1\}$
5.22	$^4A_1\{\ldots 5b_1^2 6b_1^2 7b_2^2 14a_1^2 15a_1^1 4a_2^1 \mathbf{7b_1^0} 8b_2^1\}$
5.57	$^6B_1\{\ldots 5b_1^2 \mathbf{6b_1^1} 7b_2^2 14a_1^2 15a_1^1 4a_2^1 7b_1^1 8b_2^1\}$

Table S10. The calculated VDEs for NpB_7^- at the PBE0/6-311+G*/RECP level of theory.

VDE	Final state and electron configuration
1.83	$^5A_1\{\ldots 2b_2^2 11e_1^2 12e_1^2 11a_1^1 7e_2^3 8e_2^3 13e_1^1 \mathbf{14e_1^2}\}$
4.32	$^5E_2\{\ldots 2b_2^2 11e_1^2 12e_1^2 11a_1^1 7e_2^3 \mathbf{8e_2^2} 13e_1^1 14e_1^3\}$
4.96	$^5E_1\{\ldots 2b_2^2 11e_1^2 12e_1^2 11a_1^1 7e_2^3 8e_2^3 \mathbf{13e_1^0} 14e_1^3\}$
5.30	$^7A_1\{\ldots 2b_2^2 11e_1^2 \mathbf{12e_1^1} 11a_1^1 7e_2^3 8e_2^3 13e_1^1 14e_1^3\}$
5.59	$^5A_1\{\ldots 2b_2^2 11e_1^2 12e_1^2 \mathbf{11a_1^0} 7e_2^3 8e_2^3 13e_1^1 14e_1^3\}$

Table S11. The calculated VDEs for PuB_7^- at the PBE0/6-311+G*/RECP level of theory.

VDE	Final state and electron configuration
1.81	$^6A\{…30a^2 31a^2 32a^1 33a^1 34a^1 35a^1 36a^1 \mathbf{37a^0}\}$
4.31	$^6A\{…30a^2 31a^2 32a^1 33a^1 34a^1 \mathbf{35a^0} 36a^1 37a^1\}$
4.82	$^6A\{…30a^2 31a^2 32a^1 33a^1 34a^1 35a^1 \mathbf{36a^0} 37a^1\}$
5.19	$^6A\{…30a^2 31a^2 32a^1 33a^1 34a^1 35a^1 \mathbf{36a^0} 37a^1\}$
5.76	$^6A\{…30a^2 31a^2 32a^1 33a^1 34a^1 \mathbf{35a^0} 36a^1 37a^1\}$

Table S12. The formation energies (ΔE_1 and ΔE_2, kcal/mol) of AnB_7 at the PBE0/6-311+G*/RECP theoretical level. ΔE_1 and ΔE_2 represent formation energies with charged (An^{3+}, B_7^{3-}) and neutral (An, B_7) fragments as reactants, respectively.

Species	**ΔE_1 (kcal/mol)**	**ΔE_2 (kcal/mol)**
C_{6v} PaB_7	-1137.4	-176.0
C_{6v} UB_7	-1134.1	-167.1
C_{6v} NpB_7	-1233.5	-143.1
C_{6v} PuB_7	-1214.5	-112.7

Table S13. The photoelectron and infrared spectra characteristic peaks of NpB_7 at the PBE0/6-311+G*/RECP, PBE0/6-311++G*/RECP, and PBE0/6-311+G(2df, p)/RECP theoretical levels. The values in parentheses are the changes between the results with the 6-311+G* and 6-311++G*, 6-311+G(2df, p) basis sets.

Species	Basis sets	VDD	Hirshfeld	ΔE_1	ΔE_2
C_{6v} NpB_7	6-311+G*	0.813	0.824	-1233.5	-143.1
	6-311++G*	0.793 (2.5%)	0.803 (2.5%)	-1240.8 (0.6%)	-144.3 (0.8%)
	6-311+G(2df,p)	0.788 (3.1%)	0.806 (2.2%)	-1239.2 (0.5%)	-143.6 (0.3%)

Table S14. Theoretical Cartesian coordinates (in Å) for the global minimum structures of PaB_7 at the PBE0/6-311+G*/RECP level of theory.

Atom	Coordinates (Angstroms)		
	X	Y	Z
B	0.00000000	0.00000000	-2.02033500
B	0.00000000	1.58858800	-1.46526200
B	0.00000000	-1.58858800	-1.46526200
B	-1.37575700	0.79429400	-1.46526200
B	1.37575700	-0.79429400	-1.46526200
B	1.37575700	0.79429400	-1.46526200
B	-1.37575700	-0.79429400	-1.46526200
Pa	0.00000000	0.00000000	0.59406100

Table S15. Theoretical Cartesian coordinates (in Å) for the global minimum structures of UB_7 at the PBE0/6-311+G*/RECP level of theory.

Atom	Coordinates (Angstroms)		
	X	Y	Z
B	0.00000000	0.00000000	-2.00120200
B	0.00000000	1.58850100	-1.45344000
B	0.00000000	-1.58850100	-1.45344000
B	-1.37568300	0.79425100	-1.45344000
B	1.37568300	-0.79425100	-1.45344000
B	1.37568300	0.79425100	-1.45344000
B	-1.37568300	-0.79425100	-1.45344000
U	0.00000000	0.00000000	0.58270900

Table S16. Theoretical Cartesian coordinates (in Å) for the global minimum structures of NpB_7 at the PBE0/6-311+G*/RECP level of theory.

Atom	Coordinates (Angstroms)		
	X	Y	Z
B	0.00000000	0.00000000	-1.99980200
B	0.00000000	1.58704400	-1.43967600
B	0.00000000	-1.58704400	-1.43967600
B	-1.37442100	0.79352200	-1.43967600
B	1.37442100	-0.79352200	-1.43967600
B	1.37442100	0.79352200	-1.43967600
B	-1.37442100	-0.79352200	-1.43967600
Np	0.00000000	0.00000000	0.57192800

Table S17. Theoretical Cartesian coordinates (in Å) for the global minimum structures of PuB_7 at the PBE0/6-311+G*/RECP level of theory.

Atom	Coordinates (Angstroms)		
	X	Y	Z
B	0.00000000	0.00000000	-2.01827900
B	0.00000000	1.58511400	-1.45124800
B	0.00000000	-1.58511400	-1.45124800
B	-1.37274900	0.79255700	-1.45124800
B	1.37274900	-0.79255700	-1.45124800
B	1.37274900	0.79255700	-1.45124800
B	-1.37274900	-0.79255700	-1.45124800
Pu	0.00000000	0.00000000	0.57051900